Sodium Niobate Nanowire and Its Piezoelectricity

Tsung-Ying Ke,[†] Hsiang-An Chen,[†] Hwo-Shuenn Sheu,[‡] Jien-Wei Yeh,[†] Heh-Nan Lin,[†] Chi-Young Lee,*[,†,§] and Hsin-Tien Chiu[||]

Department of Materials Science and Engineering and Center of Nanotechnology, Materials Science, and Microsystem, National Tsing Hua University, Hsinchu, Taiwan, 30043, R. O. C., Department of Applied Chemistry, National Chiao Tung University, Hsinchu, Taiwan, 30050 R. O. C., and National Synchrotron Radiation Research Center, 101 Hsin-Ann Road, Hsinchu Science Park, Hsinchu 30077, Taiwan, R.O.C.

Received: December 10, 2007; Revised Manuscript Received: March 28, 2008

Nanowires of crystalline orthorhombic sodium niobate ($NaNbO_3$), with diameters of approximately 100 nm and lengths of several to hundreds of microns, as well as cubes with edges of lengths of hundreds of nanometers were obtained by reacting niobium oxide (Nb_2O_5) with 10 and 12.5 M NaOH solutions, respectively. The microstructures of the synthesized wiry and cubic piezoelectric materials were investigated, and the details of the reactions were elucidated as well. The piezoelectricity of individual $NaNbO_3$ (*Pbma*) nanowires was confirmed by piezoresponse force microscopy, and an effective piezoelectric coefficient along the vertical direction of around a few pm/V was obtained. To our knowledge, the present work is the first report of the preparation of $NaNbO_3$ nanowires as well as the determination of piezoelectricity.

Recently, Kasuga presented the preparation of TiO_2 nanotubes by hydrothermal treatment using alkaline solutions, which have generated great interest.[1] One-dimensional metal oxides, nanotubes and nanowires have been extensively investigated in recent years.[2–5] There have been some studies on the piezoelectricity of nanowires about $BaTiO_3$, ZnO, GaN, and PZT in recent years.[6–13] Additionally, lead-free piezoelectric ceramics have received increasing interest because of their potential usefulness in environmental protection.[14–18] Among the alkali metal niobate ceramics, potassium niobate ($KNbO_3$) and $NaNbO_3$ have been studied as promising Pb-free piezoelectric ceramics.[14,19–24] However, there are two different phases of $NaNbO_3$, antiferroelectric (*Pbma*, JCPDS Card Files, No. 89−8957) and ferroelectric ($P2_1ma$, JCPDS Card Files, No. 82−0606), at room temperature.[21] To get a ferroelectric phase $NaNbO_3$ is thus an important task.[14,16,20,21,23,24] $NaNbO_3$ has attracted substantial interest among researchers and equipment designers because of its unique physical properties and its capacity to form the basis of a class of environmentally friendly materials. This investigation describes a simple wet chemical approach for preparing crystalline orthorhombic $NaNbO_3$ nanostructures in a reaction between Nb_2O_5 and concentrated NaOH solution. The morphology, structure, piezoelectric property, and formation pathway of the crystalline nanowires were studied in detail by scanning electron microscopy (SEM), transmission electron microscopy (TEM), X-ray powder diffractometry (XRD), thermogravimetry (TGA), and piezoresponse force microscopy (PFM).

In this study, Nb_2O_5 was mixed with various concentrations of NaOH solution in a Teflon reaction flask, refluxed at 120 °C for 3 h, and then cooled to room temperature. After the unreacted alkali solution had been removed, the obtained powders were washed many times using DI water before they were dried at 100 °C. Some of the powders were further annealed at 400 °C to examine their microstructure in detail before and after calcination.

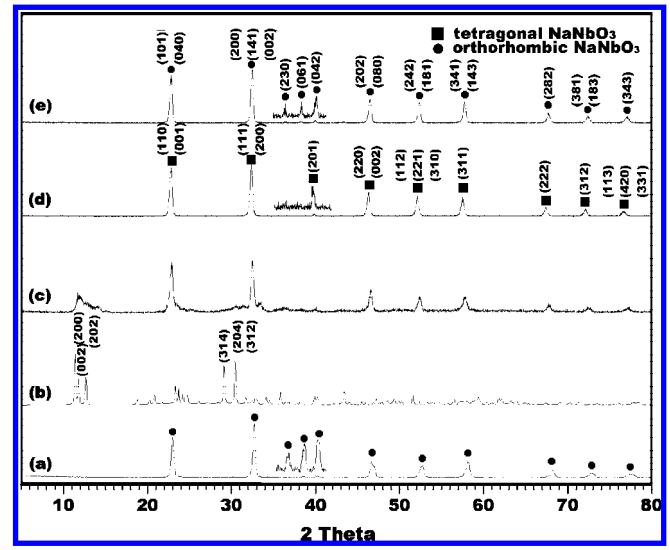

Figure 1. The XRD pattern of the powders obtained by reaction of Nb_2O_5 in various concentrations of NaOH solutions and then annealed at various temperatures. (a) The powder prepared in 12 M NaOH, and (b) the as-prepared powder obtained in 10 M NaOH. Variable temperature XRD measurement of the powder obtained in 10 M NaOH at (c) 400 °C, (d) 600 °C, (e) and cooling down to 300 °C and measured.

The morphologies of the powders were examined using a JEOL JSE-6500F field emission SEM equipped with an energy dispersive X-ray spectrometric (EDS) system to detect elements. Furthermore, crystallinity and morphological analyses were performed using a JEOL 2010 TEM. Phase detection and analysis were performed using a MAC SCIENCE MXP-3 type diffractometer with Cu Kα radiation.

Figure 1 shows the XRD study of the microstructure of the as-prepared powders and the powders after annealing. All the

* Corresponding author e-mail: cylee@mx.nthu.edu.tw.
[†] Department of Materials Science and Engineering, National Tsing Hua University.
[‡] National Synchrotron Radiation Research Center.
[§] Center of Nanotechnology, Materials Science, and Microsystem, National Tsing Hua University.
[||] National Chiao Tung University.

10.1021/jp711598j CCC: $40.75
Published on Web 05/27/2008

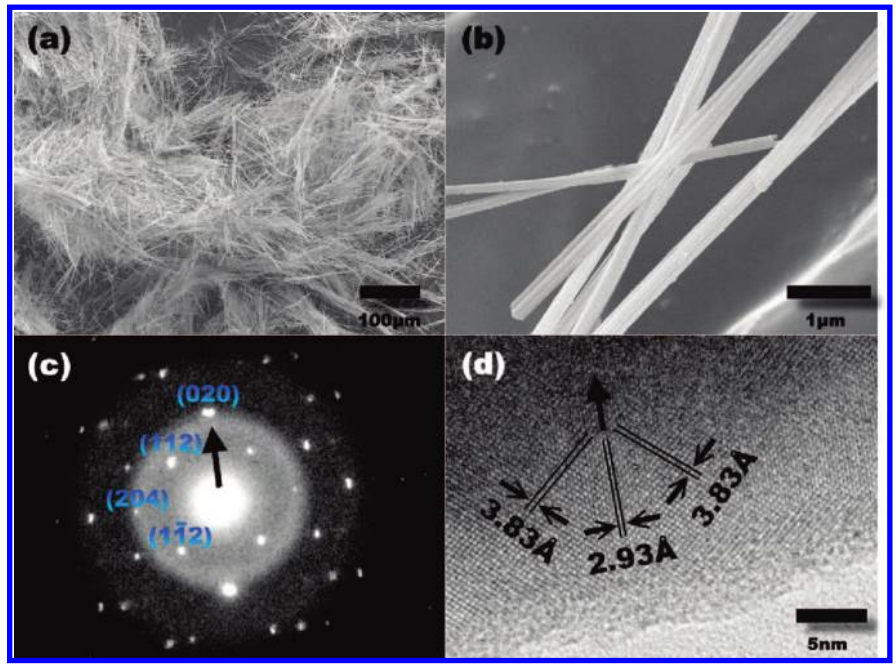

Figure 2. SEM and TEM images of the powders obtained by reacting Nb_2O_5 with 10 M NaOH solution. (a) The low magnification SEM image. (b) Enlarged view showing the bundles of the nanowires. (c) SAED of the nanowire tip, and (d) the corresponding HRTEM image of (c). (The arrows in panels c and d indicate the growth direction of this nanowire).

diffraction peaks of the as-prepared powder in 12.5 M NaOH solution (Figure 1a) are associated with orthorhombic sodium niobate. The intensities and positions of the peaks are consistent with the values in the literature. (JCPDS Card Files, No. 89−8957).

The XRD pattern of the powder obtained from the 10 M NaOH solution without further annealing is rather complex (Figure 1b). The unit cell parameters calculated by Rietveld analysis reveal that the space group of this powder material is monoclinic, *C*2/*c*, with a unit cell of $a = 17.114$ Å, $b = 5.0527$ Å, $c = 16.5587$ Å, $\beta = 113.947°$ and $V = 1308.84$ Å^3. Recently, Nyman and Xu synthesized a series of new octahedral microporous materials of composition $Na_2Nb_{2-x}M_xO_{6-x}(OH)_x \cdot H_2O$ (M = Ti, Zr; $0 < x \leq 0.4$), called Sandia octahedral molecular sieves (SOMS), using the hydrothermal method.[25−27] The framework of SMOS comprises two alternating layers. One is formed from planar edge-sharing $[NaO_{6-x}(OH_2)_x$ ($x = 1$ or 0)] octahedra, and the other consists of alternating columns of linear edge-sharing octahedra [NbO_6] and tetragonal face-sharing square-based pyramids [$NaO_3(OH_2)_2$]. All the diffraction peaks of the as-synthesized powders from the 10 M NaOH solution are attributed to SOMS with $x = 0$, $Na_2Nb_2O_6 \cdot H_2O$. The peak intensities and positions are consistent with the values presented by Nyman.[27] The TGA/DSC study of the as-synthesized powder indicated that the weight loss of this sample was 5%, corresponding to the stoichiometry of $Na_2Nb_2O_6 \cdot H_2O$ and consistent with the value of SMOS in the literature.[25] A very weak endothermic peak at about 400 °C is associated with the loss of water and the phase transformation of SMOS to perovskite sodium niobate, and an exothermic peak at 500 °C, corresponding to the orthorhombic to tetragonal phase transformation of the sodium niobate, will be described below.[28]

Figures 1b−1e present the variable temperature XRD measurements of as-synthesized powder produced in a reaction of Nb_2O_5 with 10 M NaOH solution. Figure 1b presents room-temperature XRD data concerning $Na_2Nb_2O_6 \cdot H_2O$, which is called SMOS. The XRD patterns of the powder that was heated at 400 °C were consistent with typical perovskite orthorhombic $NaNbO_3$ (Figure 1c). As the measured temperature was increased to 600 °C (Figure 1d), tetragonal $NaNbO_3$ was the major component. Additionally, as the sample was cooled to 300 °C, the thermodynamic low-temperature phase, orthorhombic $NaNbO_3$, re-emerged. These observations reveal that the phase transformation between orthorhombic and tetragonal $NaNbO_3$ occurred at 400∼600 °C, corresponding to TGA/DSC observations.

Figure 2 displays the morphologies and the microstructures of the powder obtained by reacting Nb_2O_5 with 10 M NaOH solution. Figures 2a and 2b present weakly and highly magnified SEM images of the as-synthesized powder. Many nanowires with a uniform diameter of around 100 nm and lengths of several to hundreds of microns were obtained. Figure 2c shows selected area electron diffraction (SAED) patterns that reveal the single crystalline nature of the as-synthesized powder. The pattern is associated with a [20−1] zone axis, and the nanowire direction was determined to be along the [010] axis. Figure 2d displays an HRTEM image, which includes distinct fringes. The *d* spacing values were measured to be 3.83 and 2.93 Å and were assigned to plane directions {112} and {204}, respectively. These results reveal that a singly crystalline wiry SOMS was obtained by reacting Nb_2O_5 with 10 M NaOH solution without further annealing.

However, as the concentration of the NaOH solution increased to 12.5 M, the morphology of the product changed markedly. Figure 3a presents an SEM image of the powder obtained by reacting Nb_2O_5 with a 12.5 M NaOH solution. The main products were large, sharp-edged cubes and thick plates with depths and widths of hundreds of microns and a wide range of lengths. Figure 3c shows selected area electron diffraction (SAED) patterns of the [101] zone axis, revealing the single crystalline nature of each cube. An HRTEM image in Figure 3d presents distinct fringes in the area that is marked in Figure 3b. Two planes, (040) and (10−1), were identified. The *d* spacing values were measured to be about 3.88 and 3.91 Å, equal to the values expected for orthorhombic $NaNbO_3$.

The XRD study indicates that the SOMS transferred to orthorhombic $NaNbO_3$ upon heating to 400 °C. Figure 4 presents

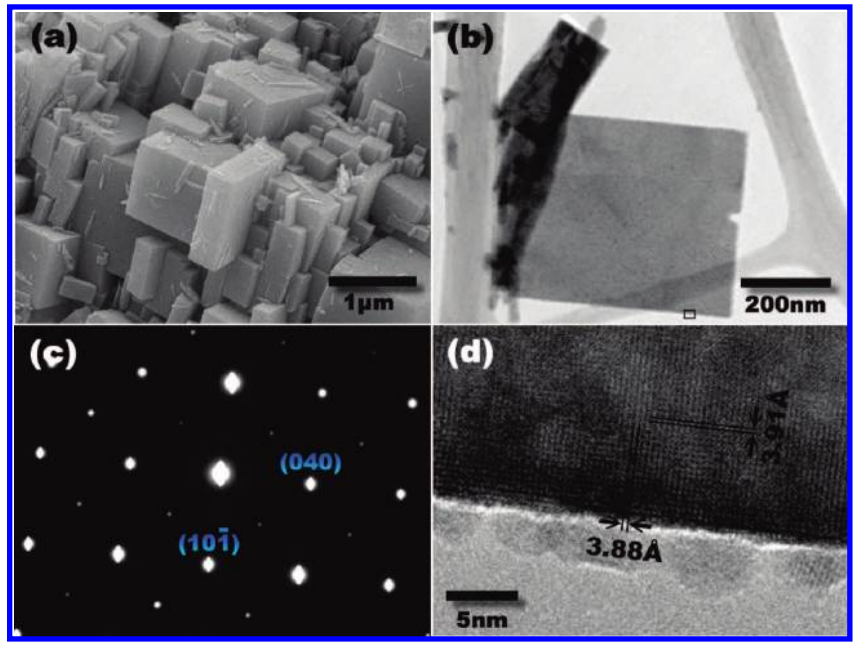

Figure 3. SEM and TEM images of the powder obtained by reacting Nb_2O_5 with 12.5 M NaOH solution. (a) The SEM image. (b) TEM image of the powder in panel a. (c) [101] zone SAED, and (d) HRTEM image of the marked rectangular region in panel b.

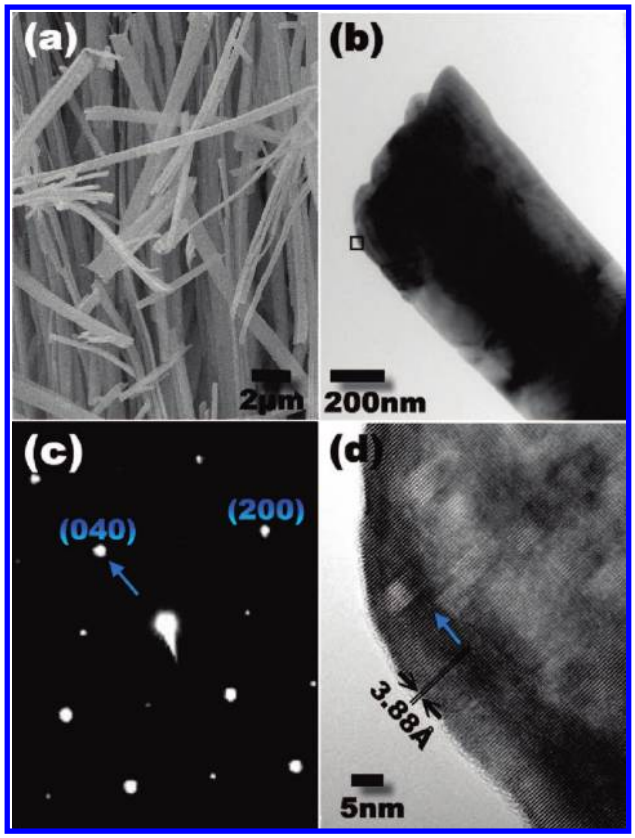

Figure 4. (a) SEM image of the prepared powder in 10 M NaOH after annealing at 400 °C, (b) TEM image of the powder in panel a, (c) [001] zone SAED, and (d) HRTEM image of the marked rectangular region in panel b. (The arrows in panels c and d indicate the growth direction of this nanowire).

the morphologies and the microstructure of the wiry SOMS following annealing at 400 °C. Figures 4a and 4b present the SEM and TEM images of the heated powder. Many nanowires with a uniform diameter of about 100 nm and lengths of several to hundreds of microns were observed. The white powders obtained before and after annealing were comprised of oxygen

SCHEME 1

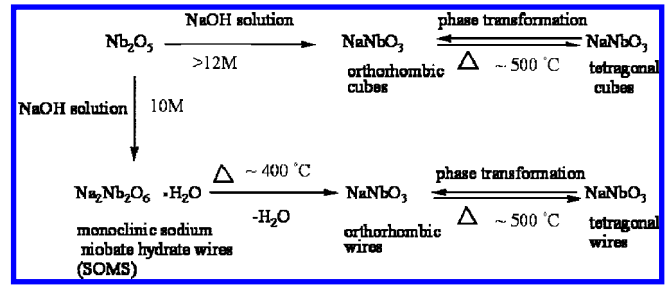

and approximately equal molar amounts of sodium and niobium, as revealed by EDS. These results show that calcination did not change the morphology and composition of the powder. According to XRD, the diffraction of the wiry SOMS following annealing at 400 °C (Figure 2c) revealed orthorhombic sodium niobate.

Figure 4c presents the SAED patterns that were marked in Figure 4b. The pattern was associated with the [001] zone axis, and the nanowire direction was determined to be [010]. Figure 4d shows an HRTEM image with distinct fringes. The *d* spacing values were measured to be 3.88 Å and were assigned to the (040) plane.

The above discussion indicates that the NaOH concentration strongly affects the morphologies and microstructures of the resulting powders obtained in the reaction of NaOH solution with Nb_2O_5. When the NaOH concentration was low (~10 M), one-dimensional sodium niobate hydrate was the first major product, and then wiry orthorhombic $NaNbO_3$ was obtained as the powder was heated to 400 °C. When the NaOH concentration exceeded 12.5 M, cubes of orthorhombic $NaNbO_3$ were formed. Further heating of the orthorhombic sodium niobate nanowires or cubes caused a phase transformation from orthorhombic to tetragonal. The results are summarized below (Scheme 1).

To measure the effective piezoelectric coefficient d_{zz} along the vertical direction of an individual $NaNbO_3$ nanowire, piezoresponse force microscopy (PFM) was employed.[29,30] The experiment was performed under ambient conditions using a

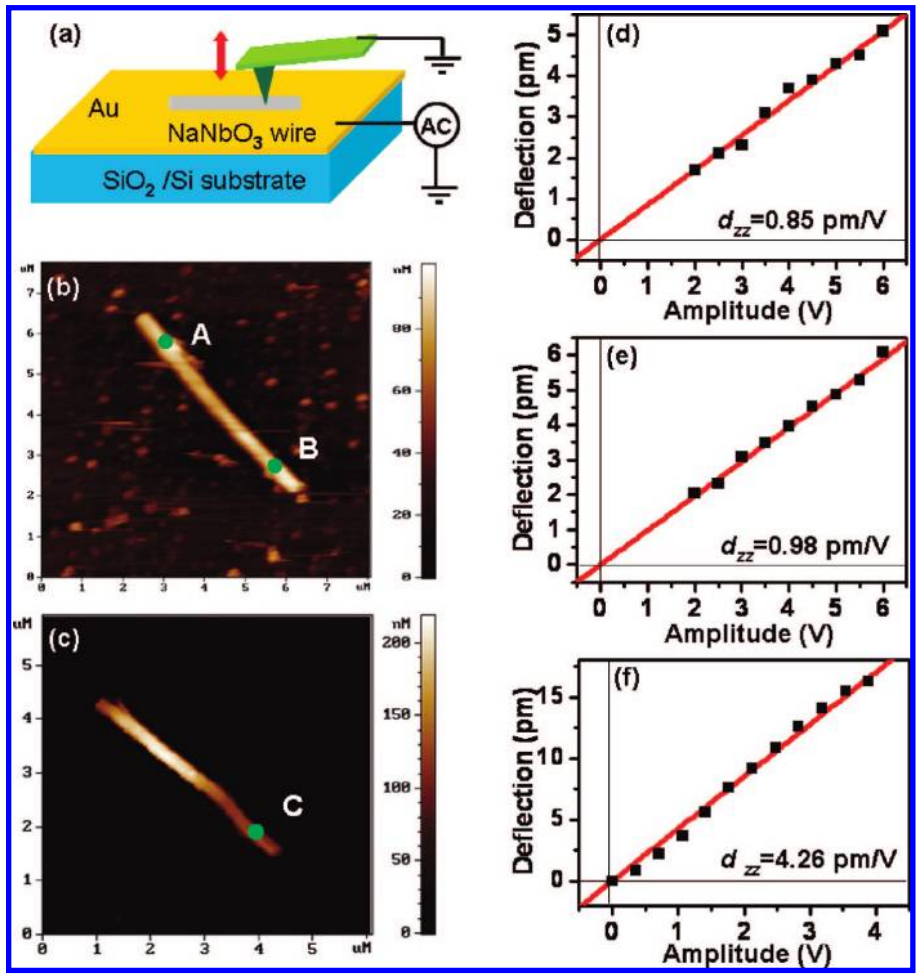

Figure 5. (a) A schematic diagram of the PFM experiment. (b and c) Topographic images of $NaNbO_3$ nanowires with widths of 200 and 100 nm and heights of 80 and 120 nm, respectively. (d−f) Deflection versus amplitude curves at the positions (d) A, (e) B, and (f) C, respectively, marked in panels b and c.

commercial atomic force microscope (AFM; Smena-A, NT-MDT). The nanowires were first dispersed on an Au film. As shown in Figure 5a, a nanowire was then found, and the AFM tip was held at various locations on the nanowire. A small alternate current (AC) voltage was applied between the Au-coated tip (NSC36/Cr−Au, MikroMasch) and the bottom Au film. The nanowire and, consequently, the tip, vibrated at the same frequency and with the same amplitude due to the converse piezoelectric effect. The d_{zz} can be determined by eq 1

$$d_{zz} = \frac{\Delta l}{V_{ac}} = \frac{D \cdot V_{pr}}{V_{ac}} \quad (1)$$

where Δl is the root-mean-square (rms) amplitude of the tip deflection, V_{ac} is the rms amplitude of the applied voltage, V_{pr} is the rms amplitude of the tip deflection voltage, and D is the AFM detector sensitivity. Details of the measurement procedure and parameters can be found elsewhere.[30]

The topographic images of two nanowires with widths of 200 and 100 nm and heights of 80 and 120 nm, respectively, are shown in Figure 5, panels b and c, respectively. The relationships between the tip deflection and the applied voltage amplitude at the locations A, B, and C marked in panels b and c in Figure 5 are shown in Figure 5, panels d−f, respectively. As expected, a linear behavior is observed in all curves. The average d_{zz} values are 0.85, 0.95 and 4.26 pm/V, respectively. As can be seen, the d_{zz} of the nanowire in Figure 5c is about four times as large as those of the nanowire in Figure 5b. The outcome suggests that a nanowire with a larger height-to-width ratio vibrates more easily under an applied electric field. Also, these values are much smaller than the piezoelectric coefficients of polarized and doped bulk $NaNbO_3$, which are about 30−40 pm/V. [20,21] Nevertheless, it should be stressed that the smaller d_{zz} values are mainly due to the fact that the electric field is applied in an unknown and unfavorable crystal direction. With proper control of the crystal orientation of the nanowires and the applied electric field, much higher values of d_{zz} can be expected. Such investigations are currently underway.

In conclusion, crystalline orthorhombic $NaNbO_3$ nanowires and cubes were synthesized by the simple base treatment of Nb_2O_5 with 10 and 12.5 M NaOH solutions. The initial major products of the reaction of Nb_2O_5 with 10 M NaOH solution were monoclinic SOMS nanowires, formed by the intercalation of NaOH to Nb_2O_5. Heating the nanowires to 400 °C yielded wiry orthorhombic $NaNbO_3$ by the removal of H_2O from the layers. The effective piezoelectric coefficient along the vertical direction of an individual $NaNbO_3$ (*Pbma*) nanowire measured by PFM is about a few pm/V. When the reaction proceeded in concentrated alkaline solution, orthorhombic $NaNbO_3$ cubes were obtained. This selective and efficient method yields specific products of the base treatment, which were perovskite materials of various shapes.

Acknowledgment. The authors like to thank the National Science Council of the Republic of China, Taiwan, for

financially supporting this research under contract Nos. NSC 93-2213-M-007-035, NSC 93-2213-M-009-003, and NSC 96-2221-E-007-100.

References and Notes

(1) Kasuga, T.; Hiramatsu, M.; Hoson, A.; Sekino, T.; Niihara, K. *Langmuir* **1998**, *14*, 3160.
(2) Han, S.; Li, C.; Liu, Z.; Lei, B.; Zhang, D.; Jin, W.; Liu, X.; Tang, T.; Zhou, C. *Nano Lett.* **2004**, *4*, 1241.
(3) Lu, W.; Lieber, C. M. *J. Phys. D* **2006**, *39*, 387.
(4) Suryavanshi, A. P.; Hu, J.; Yu, M.-F. *Adv. Mater.* **2008**, *20*, 793.
(5) Chen, M. H.; Gao, L. *Chem. Phys. Lett.* **2006**, *417*, 132.
(6) Wang, Z.; Suryavanshi, A. P.; Yu, M.-F. *Appl. Phys. Lett.* **2006**, *89*, 082903.
(7) Wang, Z. Y.; Hu, J.; Yu, M.-F. *Nanotechnology* **2007**, *18*, 235203.
(8) Wang, Z. Y.; Hu, J.; Suryavanshi, A. P.; Yum, K.; Yu, M.-F. *Nano Lett.* **2007**, *7*, 2966.
(9) Qin, Y.; Wang, X. D.; Wang, Z. L. *Nature* **2008**, *451*, 809.
(10) Wang, X. D.; Song, J. H.; Liu, J.; Wang, Z. L. *Science* **2007**, *316*, 102.
(11) Desai, A. V.; Haque, M. A. *Appl. Phys. Lett.* **2007**, *91*, 183106.
(12) Su, W. S.; Chen, Y. F.; Hsiao, C. L.; Tu, L. W. *Appl. Phys. Lett.* **2007**, *90*, 063110.
(13) Wang, J.; Sandu, C. S.; Colla, E.; Wang, Y.; Ma, W.; Gysel, R.; Trodahl, H. J.; Setter, N.; Kuball, M. *Appl. Phys. Lett.* **2007**, *90*, 133107.
(14) Saito, Y.; Takao, H.; Tani, T.; Nonoyama, T.; Takatori, K.; Homma, T.; Nagaya, T.; Nakamura, M. *Nature* **2004**, *432*, 84.
(15) Baettig, P.; Schelle, C. F.; LeSar, R.; Waghmare, U. V.; Spaldin, N. A. *Chem. Mater.* **2005**, *17*, 1376.
(16) Xie, R.-J.; Akimune, Y. *J. Mater. Chem.* **2002**, *12*, 3156.
(17) Cross, E. *Nature* **2004**, *432*, 24.
(18) Kobayashi, W.; Terasaki, I. *Appl. Phys. Lett.* **2005**, *87*, 032902.
(19) Reznichenko, L. A.; Shilkina, L. A.; Turik, A. V.; Dudkina, S. I. *Tech. Phys.* **2002**, *47*, 206.
(20) Hungria, T.; Pardo, L.; Moure, A.; Castro, A. *J. Alloy. Compd.* **2005**, *395*, 166.
(21) Reznitchenko, L. A.; Turik, A. V.; Kuznetsova, E. M.; Sakhnenko, V. P. *J. Phys.: Condens. Matter* **2001**, *13*, 3875.
(22) Ringgaard, E.; Wurlitzer, T. *J. Eur. Ceram. Soc.* **2005**, *25*, 2701.
(23) Guo, Y. P.; Kakimoto, K.; Ohsato, H. *Mater. Lett.* **2005**, *59*, 241.
(24) Cho, C.-R.; Katardjiev, I.; Grishin, M.; Grishin, A. *Appl. Phys. Lett.* **2002**, *80*, 3171.
(25) Nyman, M.; Tripathi, A.; Parise, J. B.; Maxwell, R. S.; Harrison, W. T. A.; Nenoff, T. M. *J. Am. Chem. Soc.* **2001**, *123*, 1529.
(26) Xu, H.; Su, Y.; Balmer, M. L.; Navrotsky, A. *Chem. Mater.* **2003**, *15*, 1872.
(27) Xu, H.; Nyman, M.; Nenoff, T. M.; Navrotsky, A *Chem. Mater.* **2004**, *16*, 2034.
(28) Lanfredi, S.; Lente, M. H.; Eiras, J. A. *Appl. Phys. Lett.* **2002**, *80*, 2731.
(29) Zhao, M.-H.; Wang, Z.-L.; Mao, S. X. *Nano Lett.* **2004**, *4*, 587.
(30) Lin, H.-N.; Chen, S.-H.; Ho, S.-T.; Chen, P.-R.; Lin, I.-N. *J. Vac. Sci. Technol. B* **2003**, *21*, 916.

JP711598J